Supporting Information

The Dion-Jacobson perovskite $CsSbCl_4$: a promising Pb-free solar-cell absorber with optimal bandgap ~1.4 eV, strong optical absorption ~10^5 cm^{-1}, and large power-conversion efficiency beyond 20%

Wen-hui Guo,[a] Yao-hui Zhu,*[b] Min Zhang,*[c] Juan Du,[a] Yu-lang Cen,[a] Shi-ming Liu,[a] Yong He,[a] Hong-xia Zhong,[d] Xinqiang Wang[a] and Jun-jie Shi*[a]

[a] *State Key Laboratory for Artificial Microstructures and Mesoscopic Physics, School of Physics, Peking University Yangtze Delta Institute of Optoelectronics, Peking University, Beijing 100871, China.*

[b] *Physics Department, Beijing Technology and Business University, Beijing 100048, China*

[c] *Inner Mongolia Key Laboratory for Physics and Chemistry of Functional Materials, College of Physics and Electronic Information, Inner Mongolia Normal University, Hohhot 010022, China*

[d] *School of Mathematics and Physics, China University of Geosciences, Wuhan 430074, China*

**Corresponding authors: E-mail: jjshi@pku.edu.cn; zhuyaohui@th.btbu.edu.cn; zhangm@imnu.edu.cn*

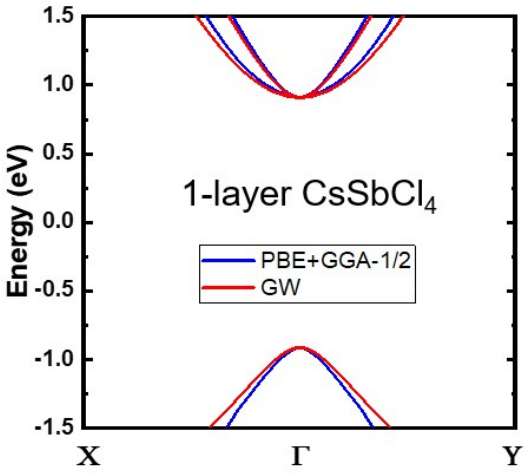

Figure S1. Electronic structures derived from PBE calculations with the GGA-1/2 bandgap modulation are in excellent consistent with the accurate and time-consuming GW calculations for the 1-layer $CsSbCl_4$. In our GGA-1/2 calculations, we chosen 8 as the value of parameter *n* for Cl^- and Sb^{3+}, then the parameter *CUT* is selected as 1.3 and 1.2 a.u. for Cl^- and Sb^{3+}, respectively.

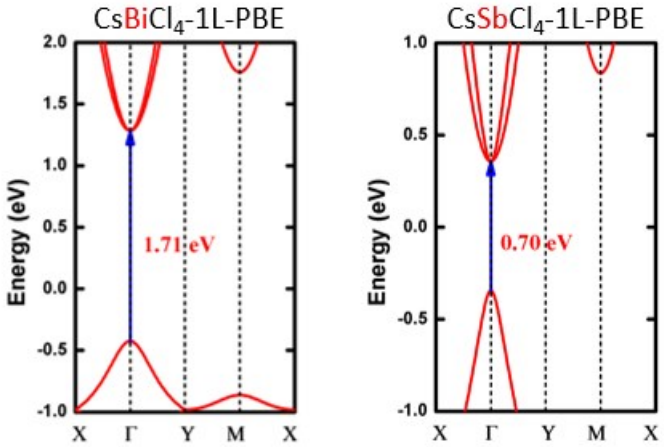

Figure S2. The electronic band structures of (a) $CsBiCl_4$ and (b) $CsSbCl_4$ 1-layer using the PBE method without SOC into account. The Bi-based DJ perovskite exhibits similar electronic dispersion to the Sb-based counterpart. However, the bandgap of $CsBiCl_4$ (1.71 eV) is much larger than that of $CsSbCl_4$ (0.70 eV). The atomic orbital energy of Bi-6*s* is clearly lower than that of Sb-5*s*, and this in turn lowers the valence band (dominated by Bi-6*s* orbitals) of $CsBiCl_4$ so as to enlarge its bandgap. Moreover, the realistic bandgap of $CsBiCl_4$ should be even larger (probably over 2 eV) since it is underestimated by the PBE functional. Therefore, $CsBiCl_4$ is not suitable for the solar-cell absorber due to its overlarge bandgap.

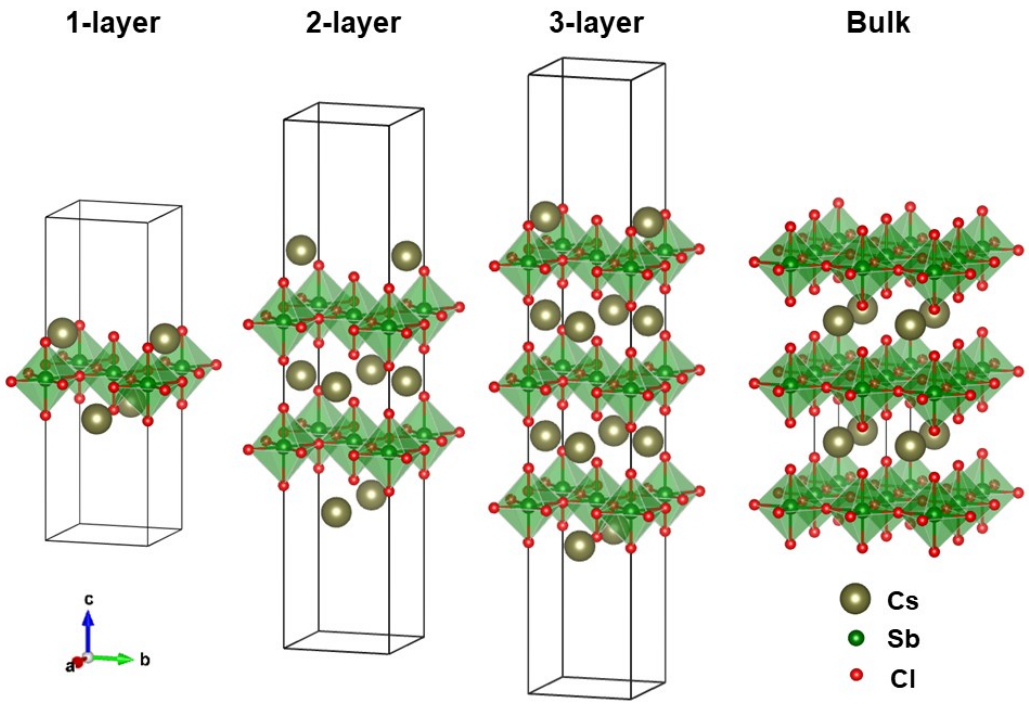

Figure S3. The crystal structures of 1-, 2-, and 3-layer and bulk $CsSbCl_4$.

Table S1. Fully optimized lattice parameter *a*, interlayer distance *d* and the single layer thickness *h* (in units of Å) in 2D layered lead-free halide perovskites $CsSbCl_4$.

Material	Layer thickness	*a*	*d*	*h*
$CsSbCl_4$	1-layer	5.36	-	5.19
	2-layer	5.36	3.66	5.19
	3-layer	5.31	3.31	5.22
	Bulk	5.28	3.30	5.25

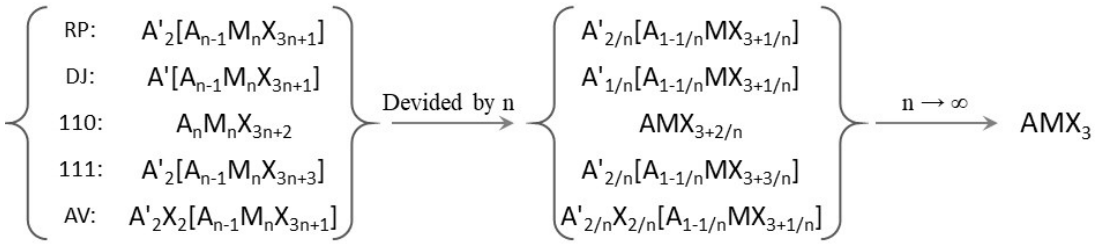

Figure S4. The 2D perovskites will be transformed into AMX_3 perovskites if the stack cycle number *n* in 2D perovskites approaches infinity.

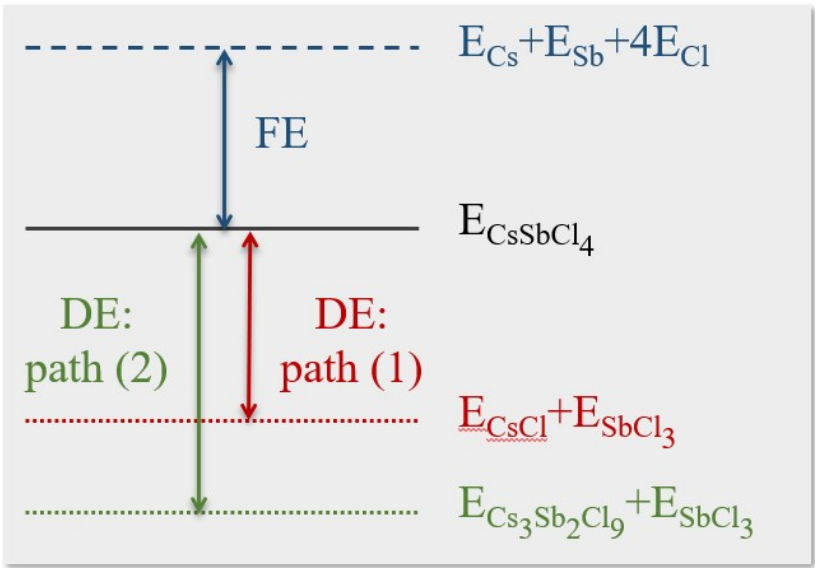

Figure S5. The schematic diagram for calculating the formation energy (FE) and decomposition energy (DE) of $CsSbCl_4$.

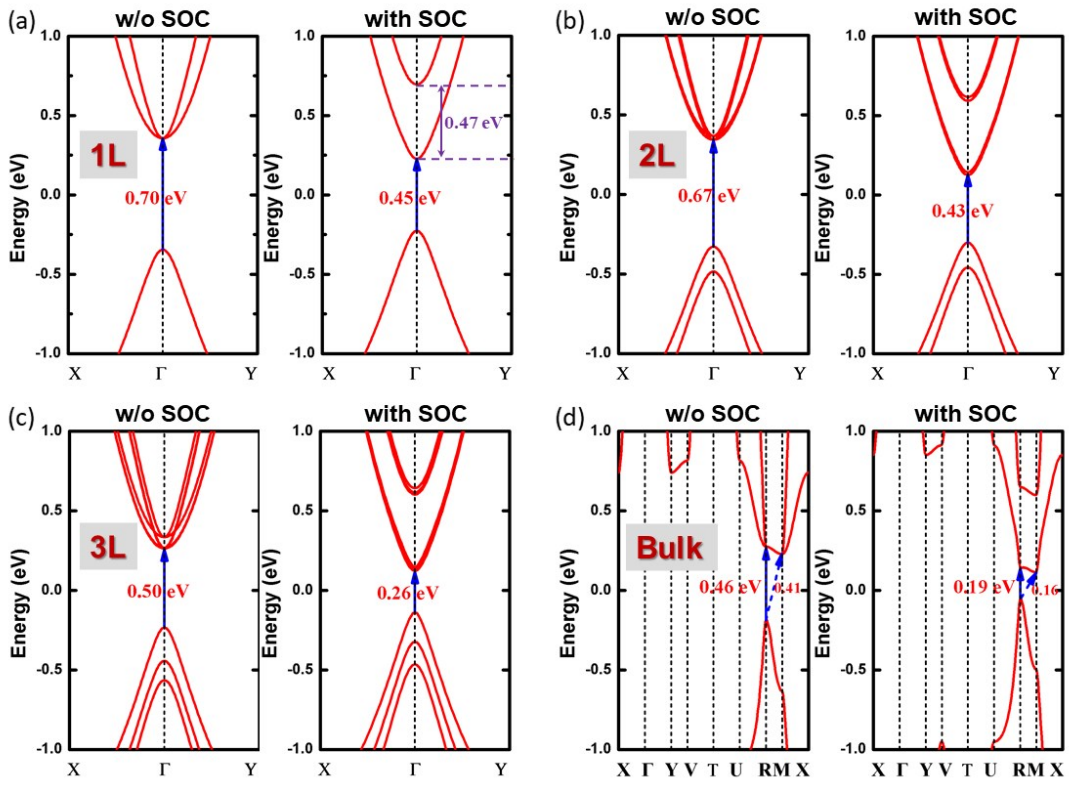

Figure S6. The electronic band structures in $CsSbCl_4$ (a) 1-layer (1L), (b) 2-layer (2L), (c) 3-layer (3L) and (d) bulk by using the PBE method, in which the right figure takes the influence of the spin-orbit coupling (SOC) into consideration.

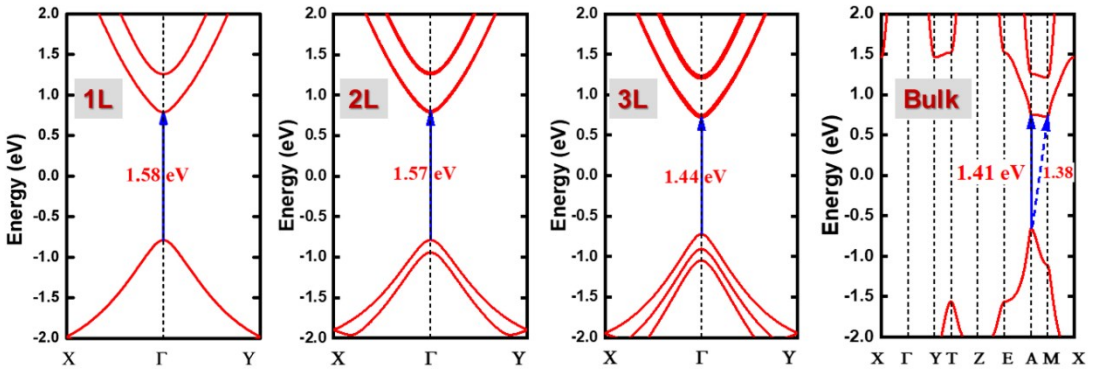

Figure S7. The electronic band structures of $CsSbCl_4$ in 1-layer, 2-layer, 3-layer and bulk configurations. Here, the band dispersions of band edge are given by PBE with the SOC effect and the bandgaps are calculated by the GGA-1/2 approach.

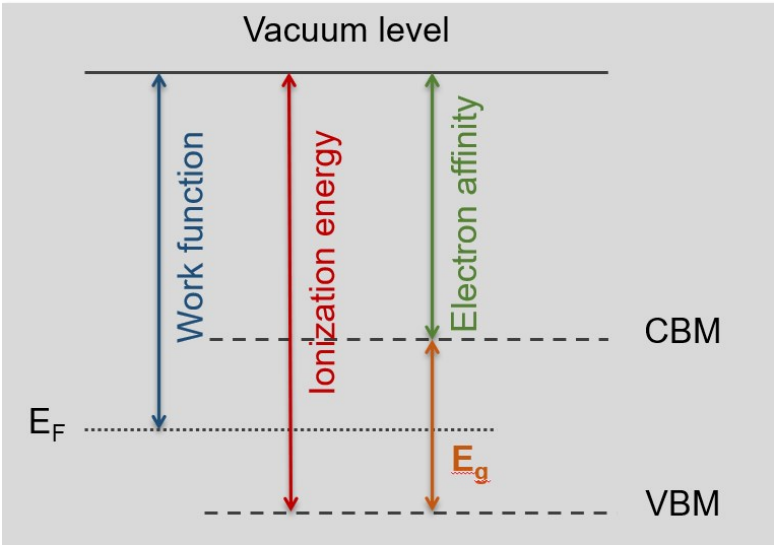

Figure S8. The schematic diagram for obtaining the band edge energy position. Here, the Fermi level E_F, work function, ionization energy, and electron affinity are also labelled.

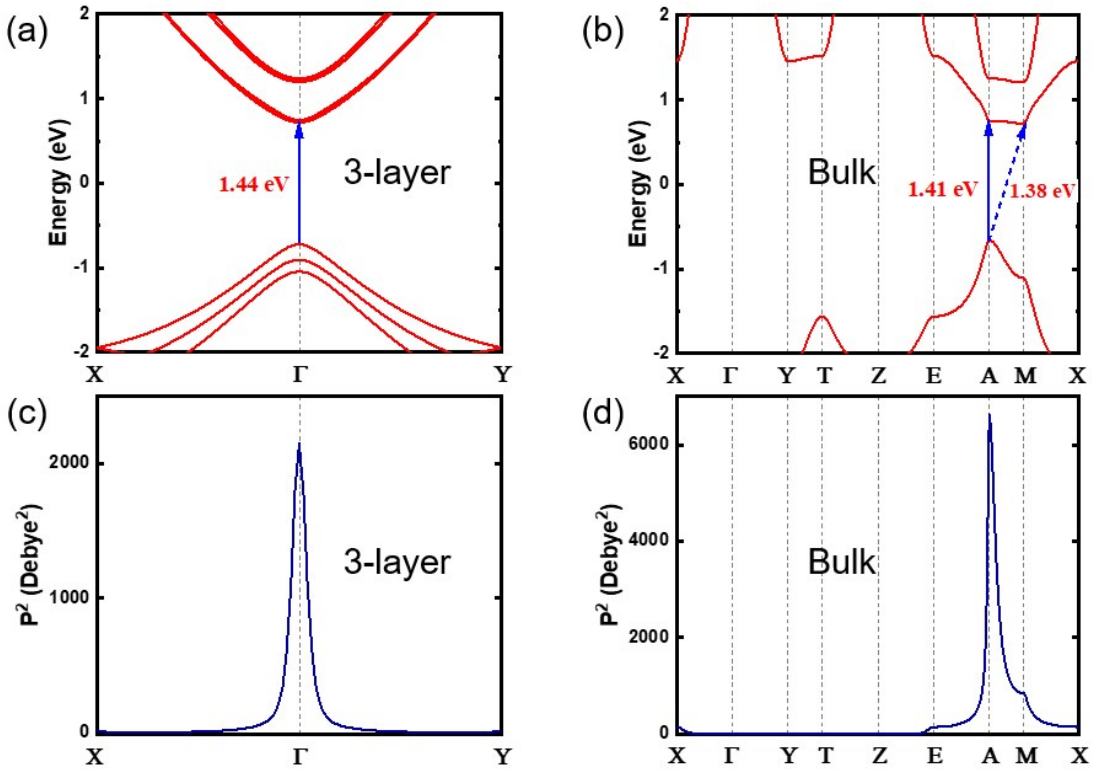

Figure S9. The band structures (a and b) and the corresponding square of the transition dipole moments between the band edges (c and d) for 3-layer (a and c) and bulk (b and d) $CsSbCl_4$.

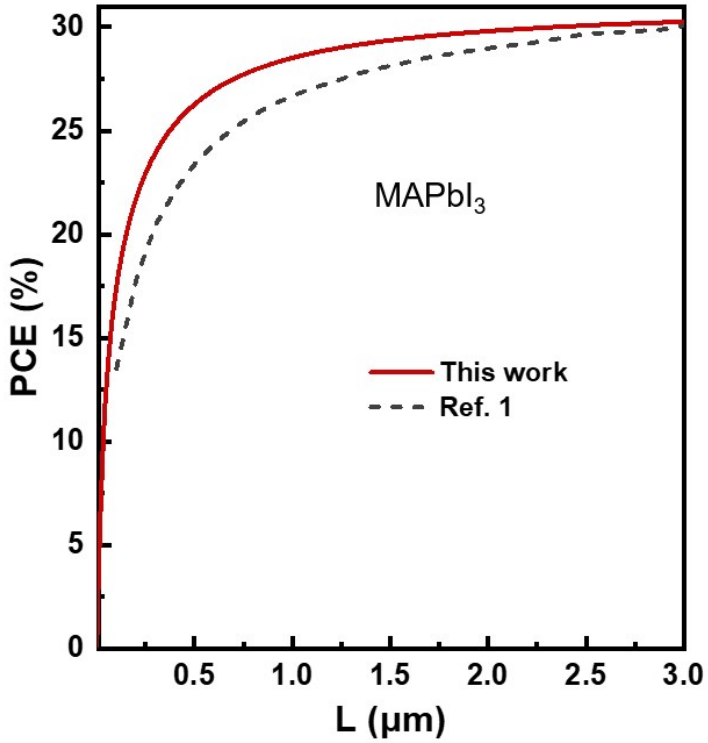

Figure S10. The calculated PCE as a function of the thickness L of the $MAPbI_3$ absorber by using the SLME method. The results in this work are in agreement with ref. 1, which indicates the accuracy of our current calculations.

Table S2. Photovoltaic device parameters of the TiO_2/$MAPbI_3$/spiro-OMeTAD junction derived from the wxAMPS code, the corresponding experimental parameters from ref. 2 are also given for comparison.

Material	Method	I_{SC} (mA/cm^2)	V_{OC} (V)	FF (%)	PCE (%)
$MAPbI_3$	wxAMPS	22.65	1.20	83.28	22.64
	Exp	23.34	1.11	77.31	20.10

Table S3. Material parameters are used in the simulation of $CsSbCl_4$- and $MAPbI_3$-based perovskite solar cells. These parameters, including thickness, carrier mobility, donor (acceptor) concentration, effective density of states, and defect density, are taken from ref. 3.

Parameters	TiO_2	Perovskite absorber	spiro-OMeTAD
Thickness (μm)	0.03	0.5	0.2
Bandgap (eV)	3.2	1.55[a], 1.41[b]	3.04
Relative permittivity	9	32[a], 10[b]	3
Electron affinity (eV)	4	3.93[a], 3.77[b]	2.11
Electron mobility ($cm^2V^{-1}s^{-1}$)	20	2[a], 501[b]	2×10^{-4}
Hole mobility ($cm^2V^{-1}s^{-1}$)	10	2[a], 22806[b]	2×10^{-4}
Donor concentration (cm^{-3})	1×10^{16}	0	0
Acceptor concentration (cm^{-3})	0	2.1×10^{17}	1×10^{18}
Effective density of states in the conduction band (cm^{-3})	2.2×10^{18}	2.2×10^{18}	2.2×10^{18}
Effective density of states in the valance band (cm^{-3})	1.8×10^{19}	1.8×10^{19}	1.8×10^{19}
Defect density (cm^{-3})	1×10^{17}	1×10^{14}	1×10^{16}

[a] Parameters of $MAPbI_3$.
[b] Parameters of $CsSbCl_4$.

References:

1. W.-J. Yin, T. Shi and Y. Yan, *Adv. Mater.*, 2014, **26**, 4653-4658.
2. S. You, H. Wang, S. Bi, J. Zhou, L. Qin, X. Qiu, Z. Zhao, Y. Xu, Y. Zhang, X. Shi, H. Zhou and Z. Tang, *Adv. Mater.*, 2018, **30**, 1706924.
3. R. Jeyakumar, A. Bag, R. Nekovei and R. Radhakrishnan, *Sol. Energy*, 2019, **190**, 104-111.